

Cation Modules as Building Blocks Forming Supramolecular Assemblies with Planar Receptor–Anion Complexes

Bin Dong,[†] Tsuneaki Sakurai,[‡] Yoshihito Honsho,[‡] Shu Seki,[‡] and Hiromitsu Maeda^{*†}

[†]College of Pharmaceutical Sciences, Ritsumeikan University, Kusatsu 525-8577, Japan

[‡]Department of Applied Chemistry, Graduate School of Engineering, Osaka University, Suita 565-0871, Japan

S Supporting Information

ABSTRACT: Ion-based materials were fabricated through ion pairing of planar receptor–anion complexes and cation modules as negatively and positively charged building blocks, respectively. Anion receptors that could not form soft materials by themselves provided mesophases upon anion binding and subsequent ion pairing with aliphatic cation modules. The mesogenic behaviors were affected by structural modification of both the cation module and the anion receptor. Synchrotron X-ray diffraction measurements suggested the formation of columnar mesophases with contributions from charge-by-charge and charge-segregated arrangements. Flash-photolysis time-resolved microwave conductivity measurements further revealed a higher charge-carrier mobility in the assembly with a large contribution from the charge-segregated arrangement than in the charge-by-charge-based assembly.

The arrangement of charged species in an appropriate fashion can potentially provide assemblies exhibiting fascinating electronic properties that cannot be observed in those comprising electronically neutral molecules.^{1,2} Charged species, electron-rich anionic and electron-deficient cationic states, can be used to form assembled structures on the basis of electrostatic attractive and repulsive interactions between opposite and identical charges, respectively. Other parameters, such as van der Waals interactions, enable the arrangement of the charged species in various packing structures in the assemblies. Therefore, the choice of charged species is essential for the fabrication of materials with unique assembled structures and resulting properties.³ As candidates for the components of ion-based materials, anion complexes of pyrrole-based π -conjugated receptors (e.g., **1a**, **1b**, **2a**, and **2b** in Figure 1a)⁴ have been shown to be planar anionic species that are suitable for the formation of assembled structures with counteranions.^{5–7} In this case, it was found that the geometries of the cationic species predominantly modulate the assembled structures. In particular, the introduction of planar cations to the receptor–anion complexes afforded charge-by-charge assemblies comprising alternately stacking positively and negatively charged species^{5a} and charge-segregated assemblies with nanoscale-segregated structures of charged species⁶ as soft materials, such as thermotropic liquid crystals. Bulky alkylammonium cations were also found to act as counterparts of the receptor–anion complexes, forming mesophases.^{5b} In these examples, the soft materials were supported by van der Waals interactions between the aliphatic

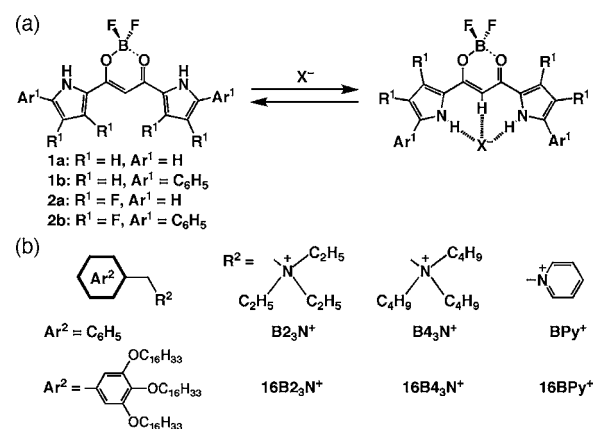


Figure 1. (a) Anion receptors **1a**, **1b**, **2a**, and **2b** and their anion-binding mode. (b) Structures of the cation modules.

3,4,5-trialkoxy-substituted aryl moieties in the receptors. In view of these studies along with the soft materials comprising modified anions,⁷ anion receptors that cannot form soft materials by themselves would afford soft materials when combined with cationic species possessing such aliphatic units. Ion-based materials formed by van der Waals interactions of modified cations as counterions of receptor–anion complexes have not been previously reported. Herein, the use of *cation modules* such as benzyltrialkylammonium chlorides ($B_nN^+Cl^-$ and $16B_nN^+Cl^-$, $n = 2$ and 4) and benzylpyridinium chlorides (BPY^+Cl^- and $16BPY^+Cl^-$) (Figure 1b) to construct ion-based supramolecular assemblies with **1a**, **1b**, **2a**, and **2b** was examined. Columnar mesophases based on charge-by-charge and charge-segregated assemblies were formed with the appropriate combinations of planar receptor–anion complexes and cation modules.

Solid-state assemblies of the receptor– Cl^- complexes with cation modules possessing unsubstituted benzyl units were revealed by single-crystal X-ray analysis (Figure 2).⁸ In the solid state of **1a**– Cl^- – B_4N^+ , a bridging CH and an inverted pyrrole NH associate with a Cl^- anion with C/N(–H)⋯ Cl^- distances of 3.919 and 3.169 Å, respectively. The other pyrrole NH at the opposite side is bound to another Cl^- anion (N(–H)⋯ Cl^- = 3.368 Å) in the absence of pyrrole inversion, resulting in a Cl^- -bridged one-dimensional (1D) chain in a perfectly linear array with a Cl^- ⋯ Cl^- distance of 9.814 Å. The dihedral angles between the core plane and the two pyrrole rings were estimated as 7.80

Received: December 14, 2012

Published: January 9, 2013

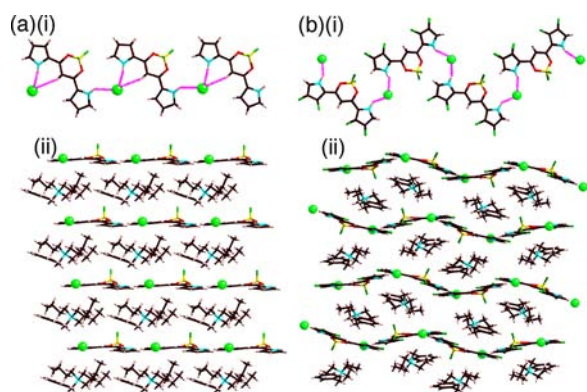


Figure 2. Single-crystal X-ray structures of (a) $1a \cdot Cl^- - B_4N^+$ and (b) $2a \cdot Cl^- - B_2N^+$: (i) Cl^- -bridged 1D chain and (ii) charge-by-charge-based packing diagram. Atom color code: brown, C; pink, H; yellow, B; yellow-green (spherical), Cl; green, F; blue, N; red, O. Solvent molecules in (b) have been omitted for clarity.

and 7.58° , indicating a fairly planar structure for the receptor. Furthermore, the charge-by-charge-based arrangement comprising alternately stacking $1a \cdot Cl^-$ and B_4N^+ layers at an angle of 3.25° with respect to the perpendicular line was observed. In the charge-by-charge assembly, the distances between $1a \cdot Cl^-$ units and between Cl^- ions are 8.011 and 8.520 Å, respectively, and the phenyl moiety in B_4N^+ is located between the uninverted pyrrole units of the receptors with distances of 4.056 and 3.695 Å. The distances between the proximal Cl^- and the cation N exhibit inequivalent values of 4.402 and 4.364 Å. The charge-by-charge assembly of $1a \cdot Cl^- - B_4N^+$ is similar to but more ordered than that of $1a \cdot Cl^- - (C_4H_9)_4N^+$,^{4a} suggesting that the introduction of a π -conjugated moiety in the cationic species is an effective way to form alternately stacking structures as observed in $1a_2 \cdot Cl^- - TATA^+$ ^{4f} and $1b \cdot Cl^- - TATA^+$,^{5a} wherein TATA⁺ is a planar triazatriangulenium cation.⁹ The solid state of the β -F derivative $2a \cdot Cl^- - B_2N^+$, contains a more planar unit, with dihedral angles of 2.46 and 3.79° between the core plane and the two pyrrole rings, neither of which is inverted. In this case, hydrogen bonds are formed only between the pyrrole NH and Cl^- , with $N(-H) \cdots Cl^-$ distances of 3.161 and 3.149 Å, possibly because of the greater polarization of the NH than in β -H derivative.^{4b} Cl^- -bridged 1D chains with a $Cl^- \cdots Cl^-$ distance of 9.895 Å and a $Cl^- \cdots Cl^- \cdots Cl^-$ angle of 115.97° are present. Moreover, a less ordered charge-by-charge assembly is formed, with a $Cl^- \cdots Cl^-$ distance of 9.250 Å and a $Cl^- \cdots Cl^- \cdots Cl^-$ angle of 125.47° in one column consisting of alternately stacking $2a \cdot Cl^-$ and B_2N^+ layers. The distances between the proximal Cl^- and the cation N also have inequivalent values of 4.949 and 4.521 Å. The phenyl moiety in B_2N^+ is located between the core plane of one receptor and the pyrrole ring of another receptor with distances

of 5.316 and 3.427 Å, respectively. In addition, there seem to be less specific interactions between the neighboring 1D chains in both complexes, except for weak $C-H \cdots Cl^-$ hydrogen bonding. The edge-to-edge stacking of the 1D chains in $2a \cdot Cl^- - B_2N^+$ can be considered as the contribution of charge-segregated assembly. It is noteworthy that the anion-binding modes with partial or no pyrrole inversion in the solid state are derived from the crystals based on cationic species with unsubstituted benzyl units and would be different from those in solution and in soft materials.

N-Based aliphatic cation-module salts $16Bn_3NCl$ ($n = 2$ and 4) and $16BPyCl$ were obtained by reacting the corresponding tertiary amines (triethylamine, tributylamine, and pyridine) with tri- $C_{16}H_{33}O$ -substituted benzyl chloride.¹⁰ Subsequently, salts of receptor- Cl^- complexes with these cation modules were prepared by evaporating solutions of the anion receptors and cation-module chlorides in 1:1 molar ratios in CH_2Cl_2 . The products were identified by 1H NMR spectroscopy and elemental analysis. The cation-module chloride salts are white solids, whereas their solid-state $[1 + 1]$ -type complexes with $1a$, $1b$, $2a$, and $2b$ are yellow, red, orange, and red solids with absorption maxima at 451/446/450, 523/514/520, 441/440/446, and 501/498/500 nm, respectively. Their solid-state emission peaks are blue-shifted relative to the anion-free receptors because stacking of the receptors is interrupted by aliphatic cation modules upon anion binding.

The Cl^- complexes of $1a$, $1b$, $2a$, and $2b$ as $16Bn_3N^+$ ($n = 2$ and 4) and $16BPy^+$ salts showed different thermal behaviors from the individual components.¹¹ The mesogenic temperature ranges varied with the structural changes of the cation modules as well as those of the anion receptors, as observed by differential scanning calorimetry (DSC) and polarized optical microscopy (POM) (Table 1). The delicate balance between the positively and negatively charged components, such as the size of the ionic part in the cation module and the substituents on the anion receptor, enabled self-organization into mesophases.^{2c,5b} During POM measurements, for example, pseudo-focal-conic fanlike, flakelike, fiberlike, and needlelike textures were observed in $1a \cdot Cl^- - 16B_2N^+$, $1b \cdot Cl^- - 16B_4N^+$, $2a \cdot Cl^- - 16B_2N^+$, and $2b \cdot Cl^- - 16B_4N^+$, respectively, upon the second heating after cooling from the isotropic liquid phase (Iso) (Figure 3).

The detailed structures were examined by synchrotron X-ray diffraction (XRD) analysis. The XRD profile of $1a \cdot Cl^- - 16B_2N^+$ at $90^\circ C$ upon second heating, which exhibited d spacings of 3.83, 2.23, 1.92, and 1.46 nm corresponding to (100), (110), (200), and (210), respectively, suggested the formation of a hexagonal columnar (Col_h) structure (Figure 4a(ii)). Its distinct difference from that at low temperature ($25^\circ C$; Figure 4a(i)) was the peak at around 0.4 nm derived from the alkyl chains, which was broad or sharp at high or low temperatures,

Table 1. Phase Transitions^a of Cation-Module Chloride Salts and Their Ion Pairs in the Presence of $1a$, $1b$, $2a$, and $2b$

receptor	$16B_2NCl$	$16B_4NCl$	$16BPyCl$
none	Cr^b 38.7 Cr^b 63.7 Col_h 129.4 ^f Iso	Cr^b 42.4 Cr^c 54.0 Cr^c 76.4 Iso [Cr^b 38.5 Col_h 81.0 Iso]	Cr^b 55.2 Cr^b 81.1 Col_h 125.9 ^f Iso
$1a$	Cr^b 50.1 Col_h 132.5 ^f Iso	Cr^d 43.8 Iso	Cr^b 54.3 Col_h 133.7 ^f Iso
$1b$	Cr^c 37.1 Cr^c 45.6 Iso [Cr^c 40.4 Iso]	Cr^b 38.6 Col_h 143.1 ^f Iso	Cr^c 48.3 Cr^c 127.3 ^f Iso
$2a$	Cr^c 6.5 Cr^b 35.7 Col_h 102.4 Iso	Cr^b 39.1 Cr^b 59.6 Cr^b 92.1 Iso	Cr^b 39.3 Col_h 53.1 ^f Iso
$2b$	Cr^c 29.1 Cr^c 51.3 Iso [Cr^c 30.7 Cr^c 49.4 Cr^c 54.1 Iso]	Cr^d 30.7 M^e 69.8 Iso [Cr^d 36.6 M^c 74.2 Iso]	Cr^b 30.2 Cr^b 45.7 Iso

^aPhases and transition temperatures (in $^\circ C$, the onset of the peak) from DSC upon second heating ($5^\circ C/min$) are listed. The entries in brackets show the transitions upon first cooling, which exhibit phases different from those upon second heating. ^bBasically as a hexagonal columnar structure. ^cUnidentified structure. ^dBasically as a lamellar structure. ^eBasically as a rectangular columnar structure. ^fValue obtained from POM measurements.

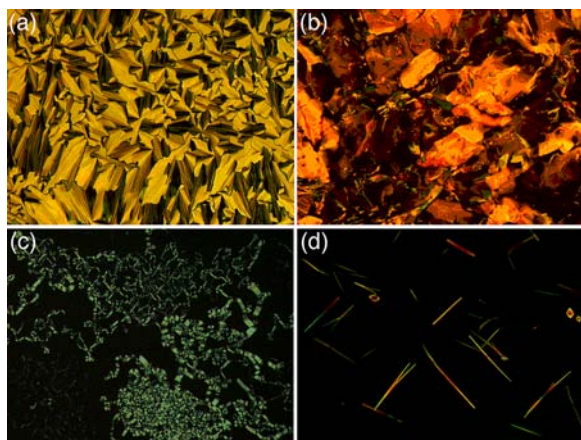


Figure 3. Representative POM textures of (a) $1a\text{-Cl}^-16B_2N^+$ at 90 °C, (b) $1b\text{-Cl}^-16B_4N^+$ at 125 °C, (c) $2a\text{-Cl}^-16B_2N^+$ at 85 °C, and (d) $2b\text{-Cl}^-16B_4N^+$ at 55 °C upon second heating after cooling from Iso.

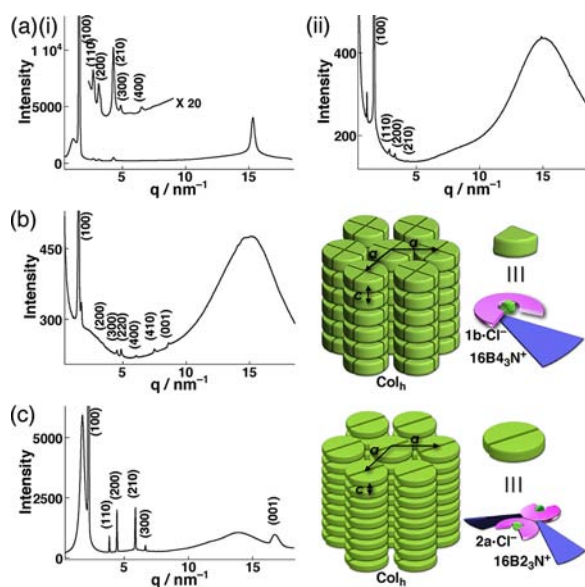


Figure 4. Representative XRD patterns of (a) $1a\text{-Cl}^-16B_2N^+$ (i) at 25 °C after once melting to Iso and (ii) at 90 °C upon second heating, (b) $1b\text{-Cl}^-16B_4N^+$ at 90 °C, and (c) $2a\text{-Cl}^-16B_2N^+$ at 85 °C upon second heating. Schematic illustrations of the assembled arrangements are shown at the right in (b) and (c). Anions are shown as green spheres, anion receptors as pink partial disks, and cation modules as fanlike shapes based on the optimized structures; the charge-by-charge and charge-segregated assemblies are represented by thick and thin disk components, respectively.

respectively. The intercolumnar distance (a) was estimated to be 4.42 nm, in accordance with the optimized structure.¹² Similarly, XRD revealed the Col_h structures in the mesophases of $1b\text{-Cl}^-16B_4N^+$ and $2a\text{-Cl}^-16B_2N^+$ (at 90 and 85 °C, respectively, upon second heating; Figure 4b,c). In contrast, $2b\text{-Cl}^-16B_4N^+$ at 55 °C upon second heating showed a complicated XRD pattern. The diffraction peaks in the low-angle regions corresponding to d spacings of 4.91, 3.60, 2.46, 1.64, 1.23, and 1.17 nm could be assigned as (200), (110), (400), (600), (800), and (810), respectively, indicating a rectangular columnar (Col_r , $C2/m$) arrangement. As previously reported, the complexes of **1a** and **1b** with dendritic anion modules (modified gallates) provided 1D lamellar mesophases with properties tuned by the

alkyl chain length in the anion module.⁷ Herein, the use of dendritic cation modules as building blocks with **1a**, **1b**, **2a**, and **2b** afforded 2D columnar mesophases, implying the importance of the ionic parts.

The (001) diffraction peak, assignable to the stacking distance between the adjacent assembled units (c), was not observed in all of the cation-module-based mesophases. In the Col_h mesophase of $1b\text{-Cl}^-16B_4N^+$ (Figure 4b), the c value of 0.74 nm implies that one assembled unit consists of four $1b\text{-Cl}^-16B_4N^+$ pairs ($Z \approx 4$ for $\rho = 0.7$; Z is the expected number of ion-pair components in a unit cell and ρ is the corresponding density) and that charge-by-charge arrangements are formed with alternately stacking cations and receptor–anion complexes, as observed in the single crystal of $1a\text{-Cl}^-16B_4N^+$.^{5,7} As for the β -F derivatives, the c value was located around 0.38 nm in $2a\text{-Cl}^-16B_2N^+$ ($Z \approx 2$ for $\rho = 1$, Col_h ; Figure 4c) and $2b\text{-Cl}^-16B_4N^+$ ($Z \approx 4$ for $\rho = 0.7$, Col_r ($C2/m$)), which is comparable to the π – π stacking distance, strongly suggesting the local stacking of identical charged species, further producing a column.⁶ The β -substituents on the anion receptors are responsible for these charge-segregated assemblies, as the fluorine moieties withdraw electrons by an inductive effect and make the intermolecular interactions among the anionic complexes sufficiently robust for stacking structures.¹³ On the other hand, the enhanced van der Waals interactions among the long alkyl chains in the cation modules also contribute to the different packing modes in the mesophases, compared with the assembled structure in the single crystal of $2a\text{-Cl}^-16B_2N^+$.

To evaluate the potential uses of ion-based materials with charge-by-charge or charge-segregated structures, flash-photolysis time-resolved microwave conductivity (FP-TRMC) measurements were performed for $1b\text{-Cl}^-16B_4N^+$ and $2a\text{-Cl}^-16B_2N^+$. This method is a powerful technique for probing the local motion of charge-carrier species.¹⁴ Kinetic traces of $\phi \sum \mu$ were obtained by TRMC (Figure 5), where ϕ denotes the

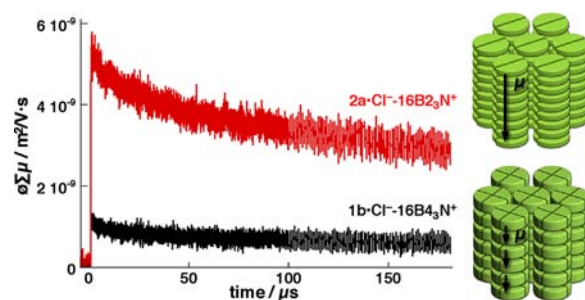


Figure 5. FP-TRMC transient signals for $1b\text{-Cl}^-16B_4N^+$ (bottom) and $2a\text{-Cl}^-16B_2N^+$ (top) at room temperature after once melting upon excitation at 355 nm with a power of 10 mW. Schematic illustrations of the motion of the charge carriers are shown at the right.

quantum yield of charge-carrier generation and $\sum \mu$ is the sum of the charge-carrier mobilities. Conductivity transients observed for both samples on a quartz plate showed a prompt rise in the signals, indicating that the singlet excited states of those compounds were responsible for free carrier generation. The maximum values of $\phi \sum \mu$ were 1.2×10^{-5} and $5.6 \times 10^{-5} \text{ cm}^2 \text{ V}^{-1} \text{ s}^{-1}$ for $1b\text{-Cl}^-16B_4N^+$ and $2a\text{-Cl}^-16B_2N^+$, respectively, suggesting that charge-segregated assemblies with a smaller stacking distance realize a higher degree of delocalization of the charge carriers along the columnar axis.¹⁵ From the ϕ values of 0.23 and 0.25% estimated from a current integration method,^{14b}

the corresponding mobilities $\sum \mu$ were calculated to be 0.05 ± 0.01 and $0.22 \pm 0.03 \text{ cm}^2 \text{ V}^{-1} \text{ s}^{-1}$ for **1b**·Cl⁻–16B₄N⁺ and **2a**·Cl⁻–16B₂N⁺, respectively. The increase in mobility for charge-segregated assemblies offers the possibility of enhancing the efficiency of charge-carrier transport in organic electronic devices.

In summary, the non-covalent association of planar anion receptors and cation-module salts afforded various supramolecular assemblies that existed as solid and soft materials. Both the ionic parts of the cation modules and the substituents on the anion receptors were powerful contributors to the modulation of the assembled structures in mesophases. Their appropriate complexation can result in charge-by-charge assemblies or charge-segregated assemblies. Derived from favorable overlap of charged π -planes, ion-based materials with charge-segregated arrangements provided charge-carrier mobility 1 order of magnitude higher than charge-by-charge-based materials, making superior electric-conducting materials. Highly ordered arrangement of charged species is a key factor to exhibit the enhanced performance. Compared with the restricted anionic species that can efficiently bind anion receptors, a variety of cationic species was more advantageous for fine-tuning ion-based assemblies comprising receptor–anion complexes and thus for preparing useful types of functional materials.

■ ASSOCIATED CONTENT

Supporting Information

Synthesis procedures and additional data. This material is available free of charge via the Internet at <http://pubs.acs.org>.

■ AUTHOR INFORMATION

Corresponding Author

maedahir@ph.ritsumei.ac.jp

Notes

The authors declare no competing financial interest.

■ ACKNOWLEDGMENTS

This work was supported by Grant-in-Aid for Young Scientists (A) (23685032) from MEXT and the Ritsumeikan R-GIRO Project (2008–2013). We thank Prof. Atsuhiko Osuka, Dr. Naoki Aratani, and Mr. Hirotaka Mori (Kyoto University) for single-crystal X-ray analysis; Dr. Noboru Ohta (JASRI/SPring-8) for synchrotron radiation XRD measurements (BL40B2 at SPring-8); Prof. Tomonori Hanasaki (Ritsumeikan University) for DSC and POM measurements; and Prof. Hitoshi Tamiaki (Ritsumeikan University) for various measurements.

■ REFERENCES

- (1) Reviews of ionic liquid crystals: (a) Binnemans, K. *Chem. Rev.* **2005**, *105*, 4148. (b) Kato, T.; Mizoshita, N.; Kishimoto, K. *Angew. Chem., Int. Ed.* **2006**, *45*, 38. (c) Greaves, T. L.; Drummond, F. J. *Chem. Soc. Rev.* **2008**, *37*, 1709. (d) Axenov, K. V.; Laschat, S. *Materials* **2011**, *4*, 206.
- (2) Examples of ion-based materials: (a) Shimura, H.; Yoshio, M.; Hoshino, K.; Mukai, T.; Ohno, H.; Kato, T. *J. Am. Chem. Soc.* **2008**, *130*, 1759. (b) Shimura, H.; Yoshio, M.; Hamasaki, A.; Mukai, T.; Ohno, H.; Kato, T. *Adv. Mater.* **2009**, *21*, 1591. (c) Goossens, K.; Lava, K.; Nockemann, P.; Van Hecke, K.; Van Meervelt, L.; Driesen, K.; Görrler-Walrand, C.; Binnemans, K.; Cardinaels, T. *Chem.—Eur. J.* **2009**, *15*, 656. (d) Ichikawa, T.; Yoshio, M.; Hamasaki, A.; Kagimoto, J.; Ohno, H.; Kato, T. *J. Am. Chem. Soc.* **2011**, *133*, 2163. (e) Wu, D. Q.; Liu, R. L.; Pisula, W.; Feng, X. L.; Müllen, K. *Angew. Chem., Int. Ed.* **2011**, *50*, 2791. (f) Ren, Y.; Kan, W. H.; Henderson, M. A.; Bomben, P. G.; Berlinguette, C. P.; Thangadurai, V.; Baumgartner, T. *J. Am. Chem. Soc.* **2011**, *133*,

17014. (g) Ichikawa, T.; Yoshio, M.; Hamasaki, A.; Taguchi, S.; Liu, F.; Zeng, X. B.; Ungar, G.; Ohno, H.; Kato, T. *J. Am. Chem. Soc.* **2012**, *134*, 2634.

(3) A recent review of ion-based materials comprising planar charged species: Dong, B.; Maeda, H. *Chem. Commun.* **2013**, DOI: 10.1039/c2cc34407f.

(4) Some examples: (a) Maeda, H.; Kusunose, Y. *Chem.—Eur. J.* **2005**, *11*, 5661. (b) Maeda, H.; Ito, Y. *Inorg. Chem.* **2006**, *45*, 8205. (c) Maeda, H.; Haketa, Y.; Nakanishi, T. *J. Am. Chem. Soc.* **2007**, *129*, 13661. (d) Maeda, H.; Bando, Y.; Shimomura, K.; Yamada, I.; Naito, M.; Nobusawa, K.; Tsumatori, H.; Kawai, T. *J. Am. Chem. Soc.* **2011**, *133*, 9266. (e) Haketa, Y.; Sakamoto, S.; Chigusa, K.; Nakanishi, T.; Maeda, H. *J. Org. Chem.* **2011**, *76*, 5177. (f) Haketa, Y.; Takayama, M.; Maeda, H. *Org. Biomol. Chem.* **2012**, *10*, 2603. (g) Haketa, Y.; Bando, Y.; Takaishi, K.; Uchiyama, M.; Muranaka, A.; Naito, M.; Shibaguchi, H.; Kawai, T.; Maeda, H. *Angew. Chem., Int. Ed.* **2012**, *51*, 7967.

(5) Examples of charge-by-charge-based soft materials: (a) Haketa, Y.; Sasaki, S.; Ohta, N.; Masunaga, H.; Ogawa, H.; Mizuno, N.; Araoka, F.; Takezoe, H.; Maeda, H. *Angew. Chem., Int. Ed.* **2010**, *49*, 10079. (b) Dong, B.; Terashima, Y.; Haketa, Y.; Maeda, H. *Chem.—Eur. J.* **2012**, *18*, 3460. (c) Bando, Y.; Sakamoto, S.; Yamada, I.; Haketa, Y.; Maeda, H. *Chem. Commun.* **2012**, *48*, 2301.

(6) Charge-segregated assemblies: Haketa, Y.; Honsho, Y.; Seki, S.; Maeda, H. *Chem.—Eur. J.* **2012**, *18*, 7016.

(7) Ion-based soft materials were prepared by complexing **1a** or **1b** with anion modules (tetrabutylammonium salts of modified gallates with aliphatic chains): Maeda, H.; Naritani, K.; Honsho, Y.; Seki, S. *J. Am. Chem. Soc.* **2011**, *133*, 8896.

(8) (a) Crystal data for **1a**·Cl⁻–B₄N⁺ (from CHCl₃/Pr₂O): C₃₀H₄₃BClF₂N₃O₂, MW = 561.93, triclinic, P1 (No. 1), *a* = 8.5203(2) Å, *b* = 9.0253(3) Å, *c* = 9.8139(3) Å, β = 84.4633(17)°, β = 86.7504(17)°, γ = 85.1185(16)°, *V* = 747.53(4) Å³, *T* = 93(2) K, *Z* = 1, *D*_{calcd} = 1.248 g/cm³, μ (Cu K α) = 1.489 mm⁻¹, *R*₁ = 0.0621, *wR*₂ = 0.1379, GOF = 0.993 (*I* > 2 σ (*I*)), CCDC 894188. (b) Crystal data for **2a**·Cl⁻–B₂N⁺ (from CHCl₃/hexane): C₂₄H₂₇BClF₂N₂O₂·1.5H₂O, MW = 576.77, monoclinic, C2/c (No. 15), *a* = 21.1495(4) Å, *b* = 16.7800(3) Å, *c* = 16.4444(3) Å, β = 114.7240(11)°, *V* = 5300.97(17) Å³, *T* = 93(2) K, *Z* = 8, *D*_{calcd} = 1.445 g/cm³, μ (Cu K α) = 1.966 mm⁻¹, *R*₁ = 0.0486, *wR*₂ = 0.1237, GOF = 1.033 (*I* > 2 σ (*I*)), CCDC 894189.

(9) (a) Laursen, B. W.; Krebs, F. C. *Angew. Chem., Int. Ed.* **2000**, *39*, 3432. (b) Laursen, B. W.; Krebs, F. C. *Chem.—Eur. J.* **2001**, *7*, 1773.

(10) (a) Percec, V.; Peterca, M.; Tsuda, Y.; Rosen, B. M.; Uchida, S.; Imam, M. R.; Ungar, G.; Heiney, P. A. *Chem.—Eur. J.* **2009**, *15*, 8994. (b) Imam, M. R.; Peterca, M.; Edlund, U.; Balagurusamy, V. S. H.; Percec, V. *J. Polym. Sci., Part A: Polym. Chem.* **2009**, *47*, 4165.

(11) The melting points of **1a**, **1b**, **2a**, and **2b** are 249.1, 298.8, 285.7, and 299.0 °C, respectively.

(12) Optimized structures of the receptor–anion complexes (ref 4a–c,e) and cation modules were obtained using Gaussian 03: Frisch, M. J.; et al. *Gaussian 03*, revision C.01; Gaussian, Inc.: Wallingford, CT, 2004.

(13) Reviews of fluorinated organic materials: (a) Babudri, F.; Farinola, G. M.; Naso, F.; Ragni, R. *Chem. Commun.* **2007**, 1003. (b) Berger, R.; Resnati, G.; Metrangolo, P.; Weber, E.; Hulliger, J. *Chem. Soc. Rev.* **2011**, *40*, 3496.

(14) (a) Saeki, A.; Seki, S.; Sunagawa, T.; Ushida, K.; Tagawa, S. *Philos. Mag.* **2006**, *86*, 1261. (b) Saeki, A.; Fukumatsu, T.; Seki, S. *Macromolecules* **2011**, *44*, 3416. (c) Saeki, A.; Koizumi, Y.; Aida, T.; Seki, S. *Acc. Chem. Res.* **2012**, *45*, 1193.

(15) (a) Feng, X.; Marcon, V.; Pisula, W.; Hansen, M. R.; Kirkpatrick, J.; Grozema, F.; Andrienko, D.; Kremer, K.; Müllen, K. *Nat. Mater.* **2009**, *8*, 421. (b) García-Frutos, E. M.; Pandey, U. K.; Termine, R.; Omenat, A.; Barberá, J.; Serrano, J. L.; Golemme, A.; Gómez-Lor, B. *Angew. Chem., Int. Ed.* **2011**, *50*, 7399. (c) Yagai, S.; Goto, Y.; Lin, X.; Karatsu, T.; Kitamura, A.; Kuzuhara, D.; Yamada, H.; Kikkawa, Y.; Saeki, A.; Seki, S. *Angew. Chem., Int. Ed.* **2012**, *51*, 6643.